A COVARIANT FORMALISM FOR THE N^* ELECTROPRODUCTION AT HIGH MOMENTUM TRANSFER

G. RAMALHO†

Centro de Física Teórica de Partículas, Av. Rovisco Pais, 1049-001 Lisboa, Portugal
†*E-mail: gilberto.ramalho@cftp.ist.utl.pt*

F. GROSS

Thomas Jefferson National Accelerator Facility, Newport News, VA 23606, USA
College of William and Mary, Williamsburg, Virginia 23185, USA

M. T. PEÑA

Centro de Física Teórica de Partículas, Av. Rovisco Pais, 1049-001 Lisboa, Portugal
Departamento de Física, Instituto Superior Técnico, 1049-001 Lisboa, Portugal

K. TSUSHIMA

EBAC in Theory Center, Thomas Jefferson National Accelerator Facility,
Newport News, Virginia 23606, USA

A constituent quark model based on the spectator formalism is applied to the $\gamma N \to N^*$ transition for the three cases, where N^* is the nucleon, the Δ and the Roper resonance. The model is covariant, and therefore can be used for the predictions at higher four-momentum transfer squared, Q^2. The baryons are described as an off-mass-shell quark and a spectator on-mass-shell diquark systems. The quark electromagnetic current is described by quark form factors, which have a form inspired by the vector meson dominance. The valence quark contributions of the model are calibrated by lattice QCD simulations and experimental data. Contributions of the meson cloud to the inelastic processes are explicitly included.

Keywords: Covariant quark model; Nucleon resonances; Meson cloud

1. Introduction

Study of the nucleon structure and its electromagnetic excitation is one of the important topics associated with the missions and activities of modern accelerator facilities. At Jefferson lab very accurate data have been

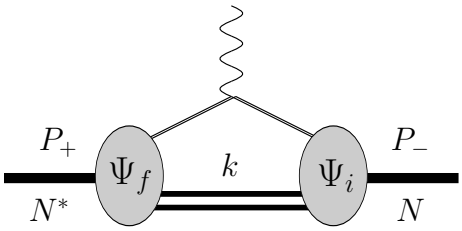

Fig. 1. $\gamma N \to N^*$ transition in the covariant spectator quark model (diquark on-shell) in relativistic impulse approximation. P_+ (P_-) represents the final (initial) baryon momentum and k the intermediate diquark momentum. The baryon wave functions are represented by Ψ_f and Ψ_i for the final and initial states, respectively.

extracted for the $\gamma N \to N^*$ reactions, for several N^* resonances at low and high Q^2 [1,2], defining new challenges for the theoretical models. Although one believes that the nucleon excitations are governed by QCD with quarks and gluons in a non-perturbative regime, it is at present nearly impossible to solve QCD exactly in the region $Q^2 = 0 - 10$ GeV^2. Thus, one has to rely on some effective and phenomenological approaches. One of popular approaches is the dynamical coupled channel reaction models [3–6], where the effective degrees of freedom are mesons and baryons. In these models a baryon core structure is assumed, and it is modified by the meson cloud dressing resulting from the meson-baryon interactions. Effective field theories based on chiral symmetry, with pions and baryons alone as degrees of freedom, are applicable only in the very low Q^2 region. On the other hand, perturbative QCD works only in the very large Q^2 region [7,8]. Alternative descriptions are constituent quark models [9]. A constituent quark has an internal structure resulting from the quark-antiquark dressing, and from the short range interaction with gluons. The quark structure of a baryon can be represented by electromagnetic valence quark form factors. In this work we present the covariant spectator quark model [7,8,10], and show several applications of the model. Covariance is important in the applications in the higher Q^2 region.

2. Spectator quark model

In the covariant spectator quark model baryons are described as a three-valence quark systems with an on-shell quark-pair, or diquark, while the remaining quark is off-shell and free to interact with electromagnetic fields. The quark-diquark vertex is then represented by a baryon B wave function Ψ_B that effectively describes quark confinement [10]. See Fig. 1.

The quark electromagnetic current j_I^μ is given by the Dirac and Pauli structures:

$$j_I^\mu = \left(\frac{1}{6}f_{1+} + \frac{1}{2}f_{1-}\tau_3\right)\left(\gamma^\mu - \frac{\not{q}q^\mu}{q^2}\right) + \left(\frac{1}{6}f_{2+} + \frac{1}{2}f_{2-}\tau_3\right)\frac{i\sigma^{\mu\nu}q_\nu}{2M_N}, \quad (1)$$

where M_N is the nucleon mass, $f_{1\pm}$ and $f_{2\pm}$ are the quark form factors as functions of Q^2, and τ_3 the isospin operator. To represent the quark structure we adopt a vector meson dominance motivated parametrization, where the form factors are written in terms of two vector meson poles:

$$f_{1\pm}(Q^2) = \lambda_q + (1-\lambda_q)\frac{m_v^2}{m_v^2+Q^2} + c_\pm\frac{Q^2M_h^2}{\left(M_h^2+Q^2\right)^2} \quad (2)$$

$$f_{2\pm}(Q^2) = \kappa_\pm\left\{d_\pm\frac{m_v^2}{m_v^2+Q^2} + (1-d_\pm)\frac{Q^2}{M_h^2+Q^2}\right\}. \quad (3)$$

In the above $m_v = m_\rho$ is a light vector meson mass that effectively represents the ρ and ω poles and M_h is the an effective heavy vector meson mass, that takes into account the short range phenomenology. We chose $M_h = 2M_N$ in the present study. The isoscalar κ_+ and isovector κ_- quark anomalous moments are fixed by the nucleon magnetic moments. The adjustable parameters are λ_q and the mixture coefficients $c_\pm$ and $d_\pm$. In the study of the nucleon properties, it turned out that $d_+ = d_-$ gives a very good description of the nucleon electromagnetic form factor [10]. This reduces the number of adjustable parameters to 4. The quality of the model description for the nucleon form factors is illustrated in Fig. 2. The quark current fixed by the nucleon form factors will be used for all other applications discussed below.

To write the baryon B wave function Ψ_B, we start from the baryon rest frame, $P = (M_B, 0, 0, 0)$, with M_B the baryon mass. We represent the baryon wave function as the direct product of the diquark and quark states of flavor, spin, orbital angular momentum and radial excitation, consistent with the baryon quantum numbers. The flavor states are written using the $\mathrm{SU}_F(3)$ quark states $\Phi_I^{0,1}$, with the diquark of total isospin $I = 0, 1$. Similarly, the diquark spin states associated with spin $S = 0, 1$, $\Phi_S^{0,1}$, can be written in terms of the polarization vectors $\varepsilon^\mu(0) = (1, 0, 0, 0)$ and $\varepsilon^\mu(\pm1) = \mp\frac{1}{\sqrt{2}}(0, 1, \pm i, 0)$, where $\lambda = 0, \pm1$ is the diquark polarization [7,10,11]. Once the wave functions are written explicitly in terms of the baryon properties in the rest frame, the relativistic generalization is performed with a boost to the moving frame. The diquark polarization vectors will be represented by a function $\varepsilon_P^\mu(\lambda)$ of the center-of-mass momentum P in the fixed-axis

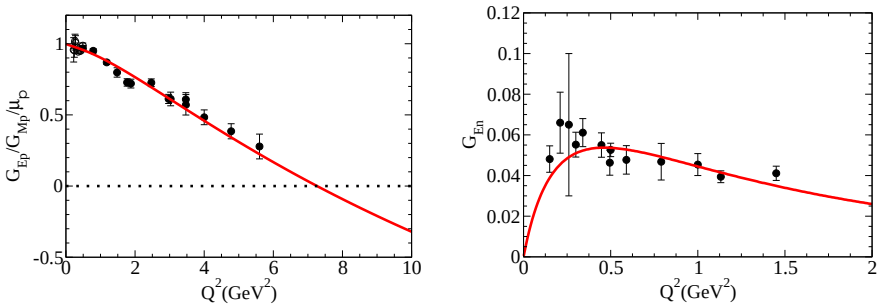

Fig. 2. Ratio for the electric and magnetic form factors for the proton, and neutron electric form factor for model II in Ref. [10]. Data are as presented in Ref. [10].

representation, as described in Ref. [11]. The explicit covariant form for the nucleon, Δ and Roper wave functions can be found in Refs. [7,8,10,12].

The electromagnetic current associated with the final state N^* in the covariant spectator quark model (see Fig. 1) is determined by

$$J^\mu = 3 \sum_\lambda \int_k \overline{\Psi}_f(P_+, k) j_I^\mu \Psi_i(P_-, k). \tag{4}$$

In the above, $\int_k$ represents the covariant integral with respect to the on-mass-shell diquark momentum and λ the diquark polarization. For simplicity, diquark and baryon polarization indices are suppressed.

3. Applications

In Eq. (4) we can write the electromagnetic transition current in terms of $q = P_+ - P_-$ and $P = \frac{1}{2}(P_+ + P_-)$. The corresponding form factors, invariant functions of Q^2, are G_E and G_M for the nucleon, G_M^*, G_E^* and G_C^* for the Δ, and F_1^* and F_2^* for the Roper.

3.1. *Nucleon*

For the nucleon, the simplest wave function has a quark-diquark S-wave configuration [10]:

$$\Psi_N = \frac{1}{\sqrt{2}} \left[\Phi_I^0 \Phi_S^0 + \Phi_I^1 \Phi_S^1 \right] \psi_N(P, k), \tag{5}$$

with $\Phi_I^{0,1}$ and $\Phi_S^{0,1}$, the diquark spin and isospin states of 0 and 1, and ψ_N a scalar wave function. Results for the nucleon form factors [10] are shown in Fig. 2. No explicit pion cloud is included for the results.

3.2. $\gamma N \to \Delta$ *transition*

The $\gamma N \to \Delta$ transition is more complex than the nucleon elastic reaction. The transition current (4), with Ψ_Δ, associated exclusively with the quark valence degrees of freedom, is insufficient to explain the data [7,8]. As near the Δ region the nucleon has enough energy to create a pion, the electromagnetic interaction with intermediate pion-baryon states should also be considered. Then, the transition form factors can be decomposed as

$$G_X^* = G_X^b + G_X^\pi, \tag{6}$$

where G_X^b stands for the contribution of the quark core (bare) and G_X^π for the contribution due to the pion cloud. The label X holds for M (magnetic dipole), E (electric quadrupole) and C (Coulomb quadrupole) form factors. This decomposition is justified when the pion is created by the overall baryon three-quark system and not from a single quark.

As a first application we describe the Δ as a quark-diquark S-state coupled to a spin 3/2 to form a total $J = 3/2$ state [7]. The transition proceeds then only through the magnetic form factor [7,8]:

$$G_M^b(Q^2) = 4\eta f_v \mathcal{I}, \tag{7}$$

where $\eta = \frac{2}{3\sqrt{3}} \frac{M_N}{M_N+M_\Delta}$, $f_v = f_{1-} + \frac{M_N+M_\Delta}{2M_N} f_{2-}$ and $\mathcal{I}$ is the overlap integral between the nucleon and Δ S-state scalar wave functions. This result allows us to understand why the pion cloud is essential to describe the data, and necessary to be added. In a pure constituent quark model the overlap integral is limited by the wave function normalization [7]. At $Q^2 = 0, \mathcal{I} \leq 1$, and for the spectator quark model this implies an upper value for $G_M^b(0)$ of 2.07, to be compared with the experimental result 3.02 [7]. Higher angular momentum partial waves for the relative quark-diquark motion are only possible to contribute to the quadrupole form factors. Since these are small compared to G_M^*, they have a reduced weight in the wave function, and consequently in G_M^*. Therefore, the discrepancy found in the leading form factor, between constituent quark models and experimental data, is mainly to be compensated by the pion cloud contributions. To adjust the valence quark contributions we use the results of the Sato-Lee model obtained from the data [3], subtracted by the pion cloud contributions. The result of the fit is presented in the left panel of Fig. 3. The experimental data points are reached when $G_M^\pi = \lambda_\pi \left(\frac{\lambda_\pi^2}{\Lambda_\pi^2+Q^2}\right)^2 (3G_D)$ is added to G_M^b (G_D the nucleon dipole factor). See the right panel in Fig. 3.

The next step is to include D-state admixtures in the wave function

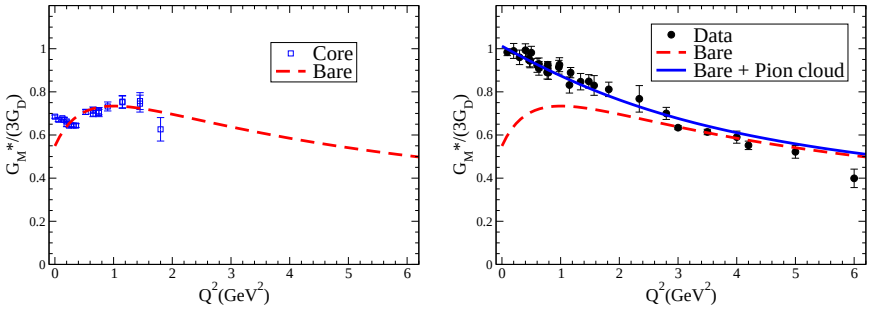

Fig. 3. G_M^* normalized by $3G_D$ in the $\gamma N \to \Delta$ transition. Left: Valence quark contributions from our model compared with the bare contributions of Sato-Lee model [3]. Right: Bare plus phenomenological pion cloud contributions, compared with the data [7].

as [8],

$$\Psi_\Delta = N\left[\Psi_S + a\Psi_{D3} + b\Psi_{D1}\right], \tag{8}$$

where Ψ_{D3} represents a D-state with a core spin 1/2 and Ψ_{D1} a D-state with a core spin 3/2. The D-state generates contributions for G_E^* and G_C^* form factors, which, otherwise for a pure S-wave function would vanish identically. To separate the valence quark contributions, we have also extended the model to the lattice QCD regime [13–15] and adjusted the D-state parameters to the quenched lattice QCD data [16] for a pion mass region where pion cloud effects are expected to be small [14]. Once the valence quark contributions are fixed from the lattice regime, the results are extrapolated back to the physical region. Finally, by adding the pion cloud contributions derived from the large-N_c limit [8,14] to the valence quark contributions G_X^b, we obtain the final result shown in Fig. 4. The results agree well with the physical data. See Refs. [8,14] for details.

3.3. $\gamma N \to$ *Roper transition*

Within the covariant spectator quark model, we can also describe the Roper system, as the first radial excitations of the nucleon [12]. Thus, the Roper wave function has the same structure as that for the nucleon Eq. (5), except for the scalar wave function, which is replaced by ψ_R. Under this assumption, the orthogonality between the Roper and nucleon wave functions is reduced to the orthogonality between the corresponding scalar wave functions: $\int_k \psi_R \psi_N = 0$ at $Q^2 = 0$. This fixes the free parameters in ψ_R completely, assuming that the nucleon and the Roper have the same short

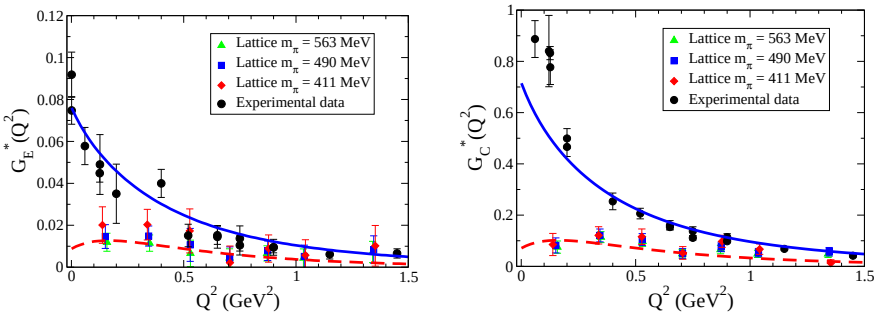

Fig. 4. Electric and Coulomb quadrupole form factor [14] for the $\gamma N \to \Delta$ transition. Lattice data are taken from [16].

range behavior, but differ in the long range structure. No extra parameter is needed additionally to the ones already fixed in the nucleon wave function [12]. Once ψ_R is defined, we can calculate and predict the nucleon to Roper transition form factors F_1^* and F_2^*. The results are shown in Fig. 5, and are consistent with the CLAS data [2] for $Q^2 > 2$ GeV^2. These facts support the idea that the valence quark degrees of freedom are well described in the covariant spectator quark model. Once the valence quark contributions are determined, we can then estimate the meson cloud contributions using the decomposition $F_i^* = F_i^b + F_i^{mc} (i = 1, 2)$, where F_i^b is the bare contribution and F_i^{mc} is the meson cloud contribution [12]. The results are also in Fig. 5.

4. Conclusions

We have developed a formalism which is successful in describing the valence quark contributions to the nucleon form factors, without the inclusion of pion cloud. The present approach also describes very well the $\gamma N \to \Delta$ data, both in the physical regime and the lattice regime, where the pion cloud effects are suppressed in the lattice regime. Furthermore, the results are consistent with the estimate of the core contributions of the Sato-Lee model. As for the $\gamma N \to$ Roper transition, we have obtained a very good description for the high Q^2 data, where valence quark degrees of freedom are expected to be dominant.

Other applications of the present approach have been made also for the determination of the Δ [17–19] and decuplet [15] electromagnetic form factors, and the octet magnetic moments (in this case including pion cloud effects).

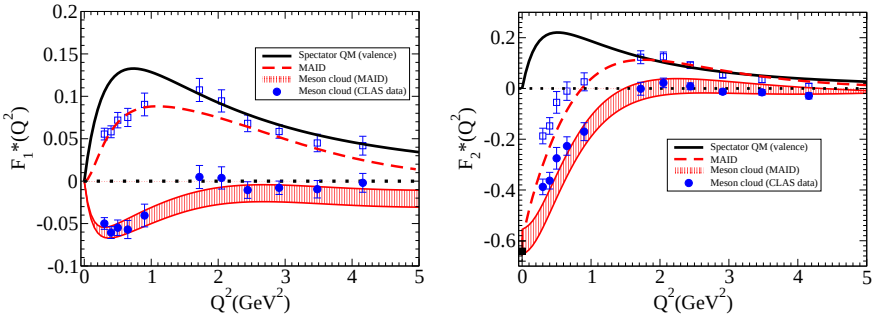

Fig. 5. $\gamma N \to$ Roper transition form factors, F_1^* and F_2^*. Data are from [2]. Meson cloud contributions based on the MAID fit [20] are represented by the band [12]. The meson cloud contributions from CLAS are also shown.

Acknowledgments:

G. R. would like to thank Viktor Mokeev for the invitation to the workshop. G. R. was supported by the Portuguese Fundação para a Ciência e Tecnologia (FCT) under the grant SFRH/BPD/26886/2006.

References

1. V. D. Burkert and T. S. H. Lee, *Int. J. Mod. Phys.* **E13**, 1035 (2004).
2. I. G. Aznauryan *et al.*, *Phys. Rev.* **C80**, p. 055203 (2009).
3. B. Julia-Diaz, T. S. H. Lee, T. Sato and L. C. Smith, *Phys. Rev.* **C75**, p. 015205 (2007).
4. S. S. Kamalov, S. N. Yang, D. Drechsel, O. Hanstein and L. Tiator, *Phys. Rev.* **C64**, p. 032201 (2001).
5. S. Schneider, S. Krewald and U.-G. Meissner, *Eur. Phys. J.* **A28**, 107 (2006).
6. A. V. Anisovich *et al.*, *Eur. Phys. J.* **A44**, 203 (2010).
7. G. Ramalho, M. T. Peña and F. Gross, *Eur. Phys. J.* **A36**, 329 (2008).
8. G. Ramalho, M. T. Peña and F. Gross, *Phys. Rev.* **D78**, p. 114017 (2008).
9. M. M. Giannini, *Rept. Prog. Phys.* **54**, 453 (1991).
10. F. Gross, G. Ramalho and M. T. Peña, *Phys. Rev.* **C77**, p. 015202 (2008).
11. F. Gross, G. Ramalho and M. T. Peña, *Phys. Rev.* **C77**, p. 035203 (2008).
12. G. Ramalho and K. Tsushima, *Phys. Rev.* **D81**, p. 074020 (2010).
13. G. Ramalho and M. T. Peña, *J. Phys.* **G36**, p. 115011 (2009).
14. G. Ramalho and M. T. Peña, *Phys. Rev.* **D80**, p. 013008 (2009).
15. G. Ramalho, K. Tsushima and F. Gross, *Phys. Rev.* **D80**, p. 033004 (2009).
16. C. Alexandrou *et al.*, *Phys. Rev.* **D77**, p. 085012 (2008).
17. G. Ramalho and M. T. Peña, *J. Phys.* **G36**, p. 085004 (2009).
18. G. Ramalho, M. T. Peña and F. Gross, *Phys. Lett.* **B678**, 355 (2009).
19. G. Ramalho, M. T. Peña and F. Gross, *Phys. Rev.* **D81**, p. 113011 (2010).
20. D. Drechsel, S. S. Kamalov and L. Tiator, *Eur. Phys. J.* **A34**, 69 (2007).